SAR IMAGE CLASSIFICATION WITH NORMALIZED GAMMA PROCESS MIXTURES

Koray Kayabol[*] *and Bilge Gunsel*

Multimedia Signal Processing and Pattern Recognition Lab.,
Istanbul Technical University, Maslak, Istanbul, Turkey
http://mspr.itu.edu.tr

ABSTRACT

We propose a novel image prior for the non-parametric Bayesian mixture model based unsupervised classification of SAR images. We modified the Normalized Gamma Process prior that constitutes a more general form of the Dirichlet Process prior in order to enclose the contribution of the adjacent pixels into the classification scheme. This yields an image classification prior embedded in a mixture model that allows infinite number of clusters and enables reaching to smoothed classification maps. Based on the classification results obtained on synthetic and real TerraSAR-X images, it is shown that the proposed model is capable of accurately classifying the pixels. It applies a simple iterative update scheme at a single run without performing a hierarchical clustering strategy as used in the previously proposed methods. It is also demonstrated that the model order estimation accuracy of the proposed method outperforms the conventional finite mixture models.

Index Terms— infinite mixture models, normalized gamma process mixtures, nonparametric Bayesian, image classification, SAR images

1. INTRODUCTION

Accurate land cover classification from high resolution Synthetic Aperture Radar (SAR) images has become an important aspect in remote sensing applications. The main problem arises from the difficulty in knowing the exact number of classes in advance. Therefore the automatic estimation of the unknown number of classes is a challenging topic in SAR image classification. We propose an unsupervised SAR image classification algorithm that models the distribution of the image intensities using a non-stationary mixture model that encloses a flexible image classification prior regarding to number of classes.

One of the traditional ways to determine the number of classes is to run the algorithms, like Expectation-Maximization (EM), several times for different model orders and resort to a criterion, like Bayesian Information Criterion (BIC). On the other hand, Bayesian approach to image classification became appealing because it allows nonparametric estimation of model order. Rather than running a fixed order mixture model several times and searching the best solution among several ones, non-parametric Bayesian approaches allow finding the solution by a single run with the help of a flexible prior. It is also known that a classification map can be improved by including the spatial information into the classification model. Under the Bayesian approach, non-stationary Finite Mixture Models (FMMs) are convenient models to incorporate the spatial interactions to model-based image classification. [1] uses a Markov Random Fields (MRFs) prior for mixture proportions to achieve a non-stationary mixture model. [2] exploits the Pólya urn model for image classification. A non-stationary latent class label model is proposed in [3] by defining a Gaussian MRF over the parameters of the Dirichlet Compound Multinomial (DCM) mixture density. [4] and [5] propose a latent Gaussian random field and link the random field to the mixture proportions by a Multinomial Logistic (MNL) function. [6] defines a MNL regression model for class labels. In [6], hierarchical agglomeration, Classification EM (CEM) and Integrated Completed Likelihood criterion are combined to obtain an unsupervised classification algorithm for SAR images.

It is shown that assuming a fixed number of mixture components limits the flexibility of FMMs. Rather than FMMs, Dirichlet Process Mixture (DPM) models allow us to work with infinite number of mixture components in the model with the help of Non-Parametric Bayesian algorithms. It appears to us that [7] is the first attempt to use DPM model for image classification. [7] combines MRFs and DP for classification. [8] proposes to apply a MRF based post-processing to the image classified by DPM model to obtain a smooth classification map. [9] describes a spatially dependent Pitman-Yor process over the superpixels which are previously segmented small image patches. In this study, we incorporate the MNL prior introduced in [10] and [6] for SAR images into a Normalized Gamma Process Mixture model (NGPM) that constitutes a more general version of the DPM model. Our motivation by using a NGPM model rather than a DPM is to obtain a smoothly segmented classification map by enclosing con-

[*]Koray Kayabol has been supported by the Scientific and Technical Research Council of Turkey (TUBITAK) under the 2232 Postdoctoral Reintegration Fellowship Programme.

tribution of the adjacent pixels into the classification scheme. This yields a normalized image prior embedded in a mixture model that enables us reaching to a smoothed classification map for the SAR images with a single run and without applying any post-processing.

The proposed SAR image classification method employs an inference scheme inspired from the Block Gibbs sampling algorithm proposed in [11] for a fast posterior inference of a truncated stick-breaking process. Unlike [11], we use Iterated Conditional Mode (ICM) updates instead of Gibbs sampling. In this way, we update the variables by their posterior modes rather than random samples that yields lower computational load.

Organization of the paper is as follows. Section 2 and 3 respectively present the proposed model and related inference algorithm. The simulation results are reported in Section 4. Section 5 summarizes the conclusion and future work.

2. NORMALIZED GAMMA PROCESS PRIOR WITH MULTINOMIAL LOGISTIC FUNCTION

We denote the pixel intensities by $x_n \in \mathrm{R}^+$ and pixel label vectors by $\mathbf{z}_n \in \{0,1\}^K$ for $n = 1, \ldots, N$. The K dimensional label vector $\mathbf{z}_n$ has the property that $\sum_{k=1}^{K} z_{n,k} = 1$ which means it indicates only one of the K classes by assigning its related element to 1. Each class has a probability density function $f(x_n|\theta_n)$ arising from a parametric family. We assign a parameter set to each pixel and assume that these parameters θ_n take values from a set $\Phi = \{\phi_1, \ldots, \phi_K\}$.

In order to include the spatial interactions into the classification model, we use the extended version of multinomial auto-logistic model proposed in [10] and [6] for SAR image classification. First, we include a new variable $\gamma_k \sim \mathrm{Gamma}(\alpha/K, 1)$ [12] into multinomial auto-logistic prior as

$$\omega_{n,k} = p(z_{n,k} = 1 | z_{\partial n,k}, \beta, \gamma_k) = \frac{\gamma_k e^{\beta v_{n,k}}}{\sum_{j=1}^{K} \gamma_j e^{\beta v_{n,j}}} \quad (1)$$

where $v_{n,k} = 1 + \sum_{m \in \mathcal{M}(n)} z_{m,k}$ and β is the smoothing parameter and $\mathcal{M}(n)$ is the set of pixels around the nth pixel. The parameter α is called the concentration parameter of the process.

When K goes to infinity, (1) yields a Normalized Gamma Process (NGP) prior,

$$G_n(\theta_n) = \sum_{k=1}^{\infty} \omega_{n,k} \delta(\theta_n - \phi_k) \quad (2)$$

where ϕ_k is distributed according to the base distribution G_0. The prior $G_n(\theta_n)$ becomes a realization from the NGP, $G_n(\theta_n) \sim NGP(\alpha, G_0, \omega_{n,1:K})$. We can write the truncated

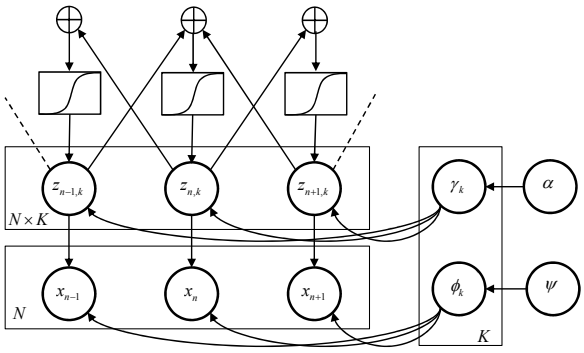

Fig. 1. Graphical representation of the proposed NGPM model with MNL regression. The graphic illustrates only three adjacent pixels for simplicity.

version of the NGP mixture (NGPM) model as follows:

$$\begin{aligned} x_n|\theta_n &\sim f(x_n|\theta_n) \\ \mathbf{z}_n|\mathbf{z}_{\partial n}, \beta &\sim \mathrm{Categorical}(\omega_{n,1}, \ldots, \omega_{n,K}) \\ \theta_n &\sim G_n(\theta_n), \\ G_n(\theta_n)|\phi_{1:K}, \alpha &\sim NGP_n(\alpha, G_0, \omega_{n,1:K}) \\ \phi_k &\sim G_0. \end{aligned} \quad (3)$$

3. POSTERIOR INFERENCE

Our aim is the intensity based SAR image classification. For this purpose, we model the class intensities using Log-Normal density which is an empirical intensity model for SAR images [13]. We choose the Log-Normal density among the other theoretical and empirical densities due to the fact that it allows us to define conjugate priors for its parameters. We define the class intensity density as a Log-Normal density denoted as $f(x_n|\phi_k) = \mathrm{LogN}(x_n|\mu_k, \tau_k)$ where

$$\mathrm{LogN}(x_n|\mu_k, \tau_k) = \frac{\sqrt{\tau_k}}{x_n\sqrt{2\pi}} e^{-\frac{\tau_k}{2}(\log x_n - \mu_k)^2} \quad (4)$$

and $\phi_k = \{\mu_k, \tau_k\}$. Hence the normal and gamma conjugate priors for μ_k and τ_k are respectively defined as

$$G_0(\mu_k, \tau_k) = \mathrm{N}(\mu_k|\mu_0, \delta/\tau_k) \times \mathrm{Gamma}(\tau_k|a, b) \quad (5)$$

where $\psi = \{\mu_0, \delta, a, b\}$ is the set of hyper-parameters. The graphical representation corresponding to the proposed model is given in Fig. 1.

In order to perform a posterior inference from the model formulated in (1)-(3) with the densities given in (4) and (5), we first marginalize out the parameters θ_n. In this way, we obtain a non-parametric model. After this collapsion, we have four key variables to infer, namely the labels $\mathbf{z}_n$, the parameters ϕ_k of the classes, the smoothing parameter β and the concentration parameter γ_k. We use the Iterated Conditional

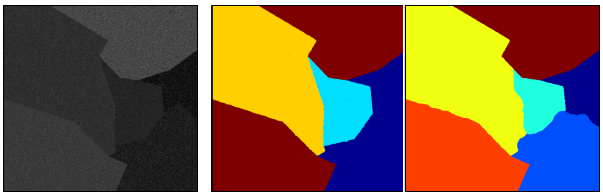

(a) (b) (c)

Fig. 2. (a) Synthetic test image, and its classification results obtained by (b) FMM-MNL-ICM and (c) NGPM-ICM.

Mode (ICM) version of the block Gibbs sampling algorithm which is proposed for posterior sampling of a stick breaking construction of a DPM model [11] to overcome the long mixing time inefficiency of the previously proposed Gibbs sampling algorithms [14]. In this way, we aim to obtain a faster algorithm than the block Gibbs sampling. We update the variables along the iterations in the following order:

$$
\begin{aligned}
\gamma_k^{t+1} &\leftarrow \max_{\gamma_k} \prod_{n=1}^{N} p(z_{n,k}^t | z_{\partial n,k}^t, \beta^t, \gamma_k) \mathrm{Gamm}(\gamma_k | \frac{\alpha^t}{K}, 1) \\
\mathbf{z}_n^{t+1} &\leftarrow \max_{\mathbf{z}_n} p(\mathbf{x}_n | \mathbf{z}_n, \phi_{1:K}^t) p(\mathbf{z}_n | \mathbf{z}_{\partial n}^t, \beta^t, \gamma_{1:K}^{t+1}) \qquad (6) \\
\beta^{t+1} &\leftarrow \max_{\beta} \prod_{n=1}^{N} p(\mathbf{z}_{1:N}^{t+1} | \beta, \gamma_{1:K}^{t+1}) \\
\phi_k^{t+1} &\leftarrow \max_{\phi_k} p(\mathbf{x}_{1:N} | \mathbf{z}_{1:N}^{t+1}, \phi_k) G_0(\phi_k | \mu_0, \delta, a, b)
\end{aligned}
$$

where $n = 1, .., N$, $k = 1, .., K$ and t is the pseudo time index. We update the concentration parameter α as follow: $\alpha^t = \alpha^{t-1} + c(\alpha_{max} - \alpha^{t-1})$ where α_{max} is the maximum value of α and c is a constant.

4. SIMULATION RESULTS

This section presents the test results obtained by the proposed and the related methods. The NGPM image prior proposed in this study is the extended version of the MNL image prior which is introduced in [10] for FMMs. To make a fair comparison of models, the same ICM update steps are used to learn both of the models. Therefore we call them briefly as NGPM-ICM and FMM-MNL-ICM methods. For the initialization of the hyper-parameters of NGPM model, we use the following scheme. We randomly select a 1000 of 7×7 image blocks over the image. In each image block, we find the Maximum Likelihood (ML) estimates of the parameters. The resulting parameter set is used to learn the hyper-parameters by ML estimation. We fix the hyper-parameters to their ML estimates and use them along the iterations. The maximum number of components in the mixture models is chosen to be 10 for each test.

In order to reveal the advantage of the NGPM prior model, we test the NGPM-ICM and FMM-MNL-ICM methods on a synthetic image SYN (see Fig. 2(a)) which has 6 different segments constituted by drawing random samples from 6 different log-normal densities. The location parameters of the log-normal densities are chosen to be close to each other to make the problem more challenging. The shape of the segments is adopted from the Prague Texture Segmentation Datagenerator and Benchmark [15]. Fig. 2(b) and 2(c) show the classification performance achieved by the proposed NGPM-ICM and the FMM-MNL-ICM methods, respectively. As seen form these classification maps, FMM-MNL-ICM collapses to a 4-class map due to the pixels having close intensities. On the other side, NGPM-ICM is able to find the exact number of classes (segments) in the test image with the help of the concentration parameter α of NGPM prior model. Setting α_{max} to a high value i.e. $\alpha_{max} = 4 \times 10^6$ prevents the collapsion of the number of classes.

Table 1. Classification recall rates (%) reported for water, urban and land areas of the real SAR image and in overall.

	water	urban	land	average
MLS [16]	89.47	35.62	84.71	69.93
FMM-MNL-ICM	99.86	99.21	40.80	79.96
AML-CEM [6]	92.36	98.29	80.97	90.54
NGPM-ICM	93.58	97.40	76.68	90.22

Along with the synthetic test image results, we show some real SAR image classification results in Fig. 3. We evaluate performance achieved by the Multi-phase Level Set (MLS) [16] which is a commonly used variational method, Amplitude density mixtures of MNL with Classification Expectation-Maximization (AML-CEM) [6], NGPM-ICM and FMM-MNL-ICM methods, on the 900×600 pixels HH polarized, TerraSAR-X SpotLight (8.2 m ground resolution) 4-look image which was acquired over the city of Rosenheim in Germany (see Fig. 3(a)). The prior image models used in both AML-CEM and FMM-MNL-ICM are the same but AML-CEM applies an hierarchical agglomerative clustering with the CEM algorithm rather than ICM and the class density used in AML-CEM is the Nakagami density rather than a log-normal. As seen from Fig. 3, NGPM-ICM algorithm provides more smooth segments than that of MLS [16]. While the NGPM-ICM method is able to find the water, urban and land areas in the image, FMM-MNL-ICM converges to an over-segmented solution. FMM-MNL-ICM results also an undesirable expansion in the urban area. Table 1 lists the numerical recall values (number of correctly classified pixels over true pixels) for water, urban and land areas. Notice that although AML-CEM uses an advance strategy that combines hierarchical agglomeration and CEM, its performance obtained at $K = 3$ is quite close to that of NGPM-ICM. However, the NGPM-ICM converges to the solution at a single run by applying simple ICM update steps without performing the hierarchical clustering as in AML-CEM.

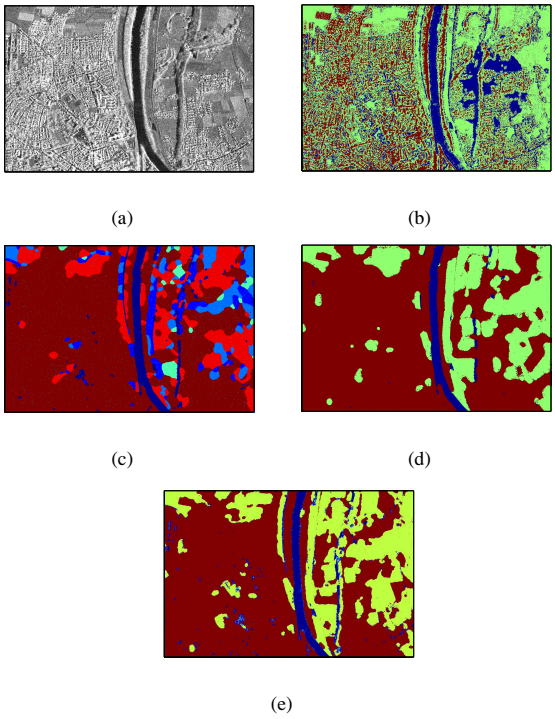

Fig. 3. (a) Real SAR image patch. Classification results obtained by (b) MLS, (c) FMM-MNL-ICM (d) AML-CEM and (e) NGPM-ICM. The TerraSAR-X image of Rosenheim (©Infoterra) was obtained from http://www.infoterra.de/.

5. CONCLUSION

In this, study we use a new flexible image prior which provides a flexibility over the number of classes for unsupervised classification of SAR images. It is shown that changing the concentration parameter of the NGPM prior, we are able to control the number of classes in the classification map. Comparing to AML-CEM which heuristically finds the solution after running CEM algorithm several times for each number of classes, the proposed method is able to converge to the solution with a single run. Additional split/merge update steps can be integrated to the ICM algorithm to improve the classification performance.

Acknowledgment

The authors would like to thank the AYIN research group from INRIA-SAM, France, (https://team.inria.fr/ayin/) for the groundtruth of SAR image and Ismail Ben Ayed for providing MLS algorithm [16] online.

6. REFERENCES

[1] S. Sanjay-Gopal and T.J. Hebert, "Bayesian pixel classification using spatially variant finite mixtures and the generalized EM algorithm," *IEEE Trans. Image Process.*, vol. 7, no. 7, pp. 1014–1028, 1998.

[2] A. Banerjee, P. Burlina, and F. Alajaji, "Image segmentation and labeling using the Polya urn model," *IEEE Trans. Image Process.*, vol. 8, no. 9, pp. 1243–1253, 1999.

[3] C. Nikou, A.C. Likas, and N.P. Galatsanos, "A Bayesian framework for image segmentation with spatially varying mixtures," *IEEE Trans. Image Process.*, vol. 19, no. 9, pp. 2278–2289, 2010.

[4] C. Fernandez and P.J. Green, "Modelling spatially correlated data via mixtures: A Bayesian approach," *J. R. Stat. Soc. B*, vol. 64, no. 4, pp. 805–826, 2002.

[5] M.A.T. Figueiredo, "Bayesian image segmentation using Gaussian field priors," in *Energy Minimization Methods Computer Vision and Pattern Recognition*, 2005, vol. LNCS 3757, pp. 74–89.

[6] K. Kayabol and J. Zerubia, "Unsupervised amplitude and texture classification of SAR images with multinomial latent model," *IEEE Trans. Image Process.*, vol. 22, no. 2, pp. 561–572, 2013.

[7] P. Orbanz and J.M. Buhmann, "Smooth image segmentation by nonparametric Bayesian inference," in *European Conf. Computer Vision, ECCV*, 2006, vol. LNCS 3951, pp. 444–457.

[8] A.R.F. da Silva, "A Dirichlet process mixture model for brain MRI tissue classification," *Medical Image Analysis*, vol. 11, pp. 169–182, 2007.

[9] E.B. Sudderth and M.I. Jordan, "Shared segmentation of natural scenes using dependent Pitman-Yor processes," in *Advances in Neural Information Processing Systems*, 2008, vol. 22, pp. 1585–1592.

[10] K. Kayabol, A. Voisin, and J. Zerubia, "SAR image classification with non-stationary multinomial logistic mixture of amplitude and texture densities," in *Int. Conf. Image Process. ICIP*, 2011, pp. 173–176.

[11] H. Ishwaran and L.F. James, "Gibbs sampling methods for stick-breaking priors," *J. Am. Statistical Assoc.*, vol. 96, no. 453, pp. 161–173, 2001.

[12] H. Yang, S. O'Brien, and D.B. Dunson, "Nonparametric Bayes stochastically ordered latent class models," *J. Am. Statistical Assoc.*, vol. 106, no. 495, pp. 807–817, 2011.

[13] C. Oliver and S. Quegan, *Understanding Synthetic Aperture Radar Images*, Artech House, Norwood, 1998.

[14] R.M. Neal, "Markov chain sampling methods for Dirichlet process mixture models," *J. Comp. Graph. Stat.*, vol. 9, no. 2, pp. 249–265, 2000.

[15] M. Haindl and S. Mikes, "Texture segmentation benchmark," in *Int. Conf. Pattern Recognition, ICPR*, 2008, pp. 1–4.

[16] C. Vazquez, A. Mitiche, and I. Ben Ayed, "Image segmentation as regularized clustering: a fully global curve evolution method," in *Int. Conf. Image Process. ICIP'04*. IEEE, 2004, pp. 3467–3470.